Flexural Strengthening of Corrosion-damaged RC Bridge Piers Using Ultra-High-Performance Concrete Layers: An Experimental Study

Biswas Rajib Kumar*　Takashi Misawa**　Takahiro Saito*

Abstract

We developed a method for strengthening RC bridge piers affected by corrosion damage. We examined five single-shaft RC bridge piers of the same dimensions and rebar configuration under reversed cyclic loading, in which we applied axial stress of 1 MPa to the specimens. Of the five specimens, two specimens underwent an average of 10% rebar corrosion (Group 1); another two specimens underwent an average of 15% rebar corrosion (Group 2); and one specimen served as the control. We retrofitted one specimen from each group with ultra-high-performance concrete (UHPC) layers measuring 50 mm in thickness. The results showed that corroded specimens strengthened with UHPC layers exhibit superior structural performance: for example, the maximum load carrying capacity (MLC) of the 15% corroded specimen increased by 24% compared to the sound specimen. Our results show that the proposed approach is highly effective in strengthening corrosion-damaged RC bridge piers.

Keywords: UHPC, strengthening, cyclic loading, rebar corrosion

1. Introduction

Bridges are essential components of the social infrastructure and significantly affect the national economy. Bridges located in marine environments are often exposed to corrosion damage. Given the cost of demolition and reconstruction and associated traffic congestion, replacing an entire damaged bridge may not be feasible. Strengthening damaged bridges is a possible alternative; developing a reliable method for strengthening damaged bridges would represent a major breakthrough.

UHPC is a new construction material that offers structural properties superior to conventional concrete. UHPC offers modulus of elasticity, compressive strength, and tensile strength exceeding 44 GPa, 155 MPa, and 19 MPa, respectively,[1] making it an ideal strengthening material for damaged reinforced concrete structures.

Yuan et al.[2] examined the strengthening effects of UHPC jackets on the cyclic response of RC bridge piers. The results showed that a UHPC jacket significantly improves strength and stiffness. Dadvar et al.[3] examined a strengthening technique involving UHPC jacketing for circular RC columns. The results showed that UHPC jackets significantly increase load-carrying and energy absorption capacity.

Little is currently known about strengthening corrosion-damaged RC bridge piers using UHPC layers. To address this research gap, we sought, in this study, to develop a strengthening scheme for corrosion-damaged RC bridge piers that would restore structural performance without affecting the original geometry. We used UHPC, an advanced strengthening material, to enhance the structural performance of the corroded RC bridge piers. We examined five single-shaft RC bridge piers, including sound, corroded, and retrofitted specimens, under reversed cyclic loading. Important performance indices for evaluating the performance of the strengthening scheme included MLC, ductility, stiffness degradation, energy absorption, and curvature. The results obtained from this study should prove useful in formulating strategies for maintaining corrosion-damaged RC bridge piers.

2. Experimental study

2.1 Specimens

Our investigation included five single-shaft RC bridge piers, fabricated to the same dimensions and reinforcing configurations. The specimens were cast with a height of 1,650 mm and a square cross-section of 400 mm, along with a footing with dimensions measuring 1,500 mm x 1,500 mm x 850 mm. Each specimen was reinforced with 16 mm deformed reinforcing bars. The reinforcement ratio for the longitudinal rebars was 2%. We used 13 mm deformed reinforcing bars as stirrups. The specimens were designed in accordance with the design code of the Japan Society of Civil Engineers (JSCE, 2007).[4] The reinforcement details can be seen in Figure 1(a). The RC bridge pier specimens were subjected to combined

*技術本部技術研究所土木研究グループ　**技術本部技術研究所

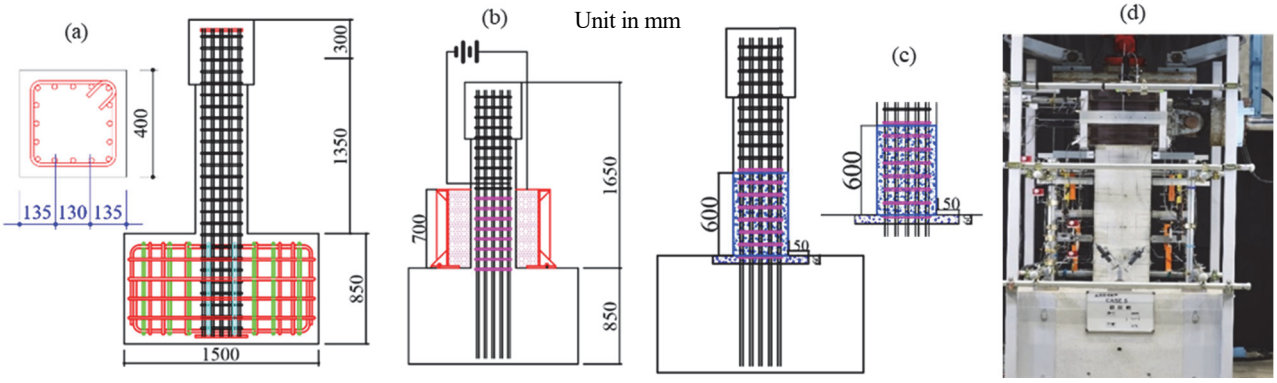

Figure 1. (a) Specimen details (b) Corrosion setup (c) Location of UHPC layer (d) Photo of experimental setup

axial and reverse cyclic loading. During the reversed cyclic loading, an axial force of 160 kN (1 N/mm^2) was applied to each of the five specimens. Of the five specimens, Case 1 was used as the control specimen; Cases 2 and 3 were subjected to 10% rebar corrosion; and Cases 4 and 5 were subjected to 15% rebar corrosion (see Table 1).

2.2 Material properties.

UHPC, deformed rebar, and normal concrete were the materials used in the experimental study. Initially, the specimens were fabricated with concrete with an average compressive strength of 25 MPa. The 28-day average tensile strength of concrete was determined to be 1.7 MPa; the elastic modulus of the normal concrete was determined to be 29.5 GPa; and the yield strength of longitudinal reinforcements (D16) and stirrups (D13) was determined to be 390 and 383 MPa, respectively. UHPC was used to strengthen two corroded specimens. The mix proportion of the UHPC used in the experiment was 185:1108:1129:154:12.2 for water: cement: sand: metal fiber: water reducing admixture. In the UHPC mix, we used only one type of steel fiber. The straight fibers were 20 mm in length and 0.2 mm in diameter. The 28-day compressive and tensile strength of UHPC was 143 MPa and 13.7 MPa, respectively. Based on the results, the elastic modulus and Poisson ratio, respectively, were determined to be 51.8 kN/mm^2 and 0.22.

Corrosion process

After the fabrication and curing of the test specimens, we performed accelerated corrosion testing. The targeted area for rebar corrosion was enclosed with a plastic tank, as shown in Figure 1(b). This tank was filled with a 5% NaCl solution. Copper plates were placed around the specimen; these steel plates were connected to the negative terminal of the power supply and used as cathodes. Longitudinal rebars were connected to the positive terminal and used as anodes. Since the study goal was the flexural strengthening of corrosion-damaged RC bridge piers, we prevented corrosion of the stirrups using suitable paints, while the longitudinal rebars were connected to the positive terminal of the power supply and used as anodes. The electric current was 0.5 mA/cm^2 during the corrosion process. Since corrosion damage at the connection point between pier and footing is understood to be more important due to potential plastic hinge formation, we limited corrosion damage to a height of 600 mm above the footing. The time required to achieve the desired rebar corrosion was determined by the following equation:

$$t(sec) = \frac{m_{loss} \cdot n_{specimen} \cdot C_{Faraday}}{Current(amp) \cdot M_{specimen}} \quad (1)$$

where C_F = 96500 C/mol; m_{loss} = required mass loss; $n_{specimen}$ = 2; and $M_{specimen}$ = 55.8 mol

Table 1: Experimental cases, corrosion ratio and crack width

Group	Cases	Remark	Corrosion ratio (%)	Max. corrosion ratio (%)	Maximum crack width
	Case 1	Sound	0		0
Group 1	Case 2	10% cor.	10	12.9	0.2
	Case 3	10% cor.& retrofitted with UHPC	10.1	13	0.15
Group 2	Case 4	15% cor.	14.7	20.4	0.5
	Case 5	15% cor.& retrofitted with UHPC	15.6	19.5	0.2

Experimental setup

After the corrosion process, the whole concrete cover in the corroded area of Cases 3 and 5 was removed by water jet. The specimens were retrofitted with UHPC layers measuring 50 mm in thickness. The location of the UHPC layers can be seen in Figure 1(c). The experimental setup used for the reverse cyclic loading can be seen in Figure 1(d). The specimens were connected to the rigid foundations of the experiment room with eight threaded rods. Specimens were connected to vertical and horizontal hydraulic jacks to apply axial and lateral forces. The loading scheme commenced with the application of an axial load: The specimens were subjected to a constant axial stress of 1 MPa, which is equivalent to 160 kN. After the application of axial force, the specimens were subjected to reversed cyclic loading with a drift ratio ranging from 0.25% to 8%, as shown in Figure 2. Load cells were mounted in the hydraulic jacks to measure applied loads. Horizontal and vertical displacements were measured using linear variable displacement transducers (LVDTs). A total of 27 LVDTs were deployed to measure vertical and horizontal displacement. Strain gauges in the steel bars were used only in the sound specimen; they were omitted from the other specimens because the rebars were damaged by electric corrosion.

RESULTS AND DISCUSSION

Corrosion-induced cracking

In the corrosion process, corrosion products appear on the steel bar, with the amount of corrosion products continuing to grow. As the amount of corrosion product increases, it exerts pressure on the surrounding concrete, generating cracks in the concrete cover. The crack widths of the corroded specimens increased considerably with the increase in corrosion ratio. In general, corrosion cracks emerged parallel to the longitudinal rebars. The maximum crack widths recorded for Cases 2, 3, 4, and 5 were 0.2 mm, 0.15 mm, 0.5 mm, and 0.2 mm, respectively.

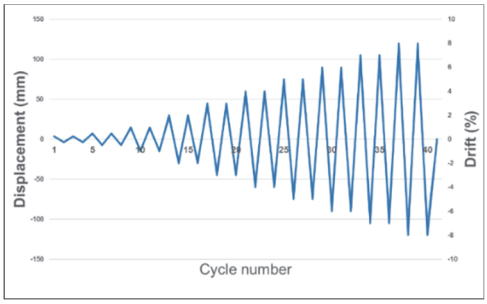

Figure 2. Quasi-static cyclic loading history

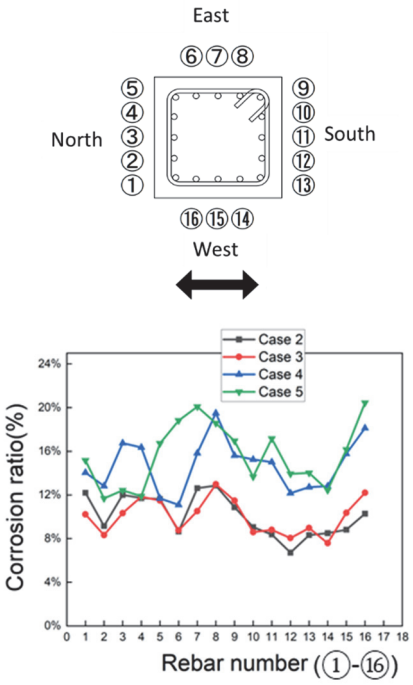

Figure 3. Mass loss of the longitudinal rebars

Corrosion process

Following the loading test, the longitudinal rebars in the corroded area were removed from the concrete to determine the extent of the corrosion**.** Next, to eliminate the corrosion products, we submerged the rebars in a 10% diammonium hydrogen citrate solution at 60 ℃. Figure 3 presents the corrosion distribution for Cases 2 to 5. Each rebar was assigned a unique number. Since the corrosion process in this study was induced by chloride, corrosion occurred in a non-uniform manner. The average mass loss or corrosion ratio was determined to be 10.1%, 10.0%, and 15.6%, and 14.7% for Case 2, Case 3, Case 4 and Case 5, respectively. In Case 2, the maximum and minimum corrosion ratios of a single rebar were determined to be 12.9% and 6.7%; in Case 3, these were determined to be 13.0% and 7.6%. In Case 4, the maximum and minimum corrosion ratios were determined to be 20.4% and 11.7%; in Case 5, the maximum and minimum corrosion ratios were determined to be 19.5% and 11.1%, respectively. The differences between the maximum and minimum corrosion ratios in Cases 2, 3, 4, and 5 were determined to be 48%, 42%, 43%, and 43%, respectively. Table 1 summarizes the various corrosion ratios and crack widths. Note that corrosion pit depth increases with increasing corrosion ratio. The average pit depths obtained for Cases 2, 3, 4, and 5 were 1.0, 0.9, 1.2 and 1.1 mm, respectively.

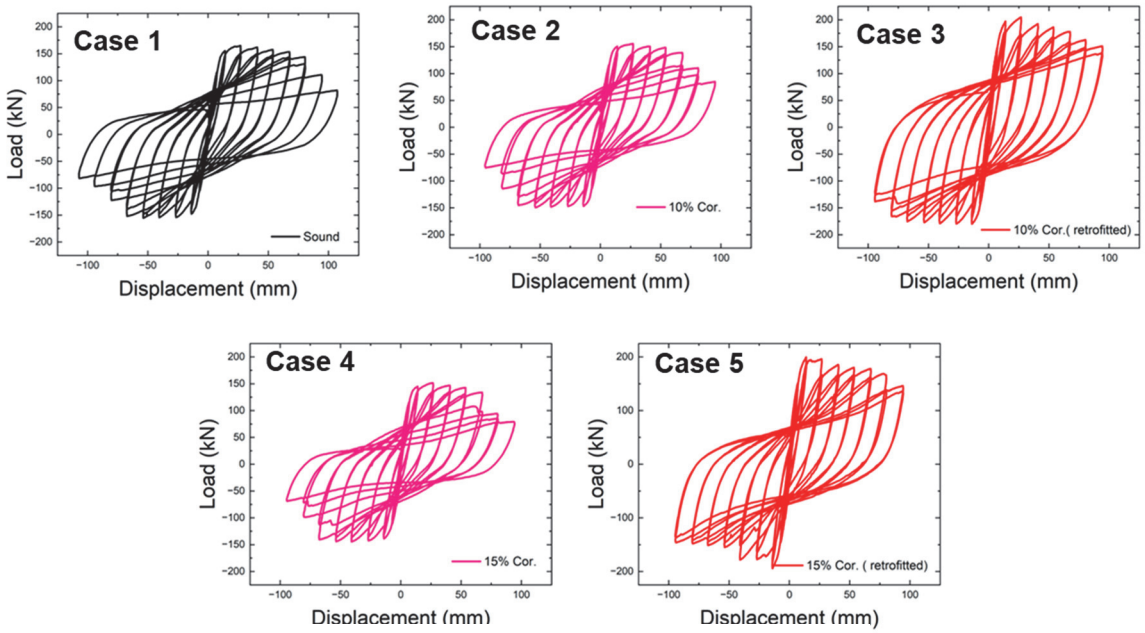

Figure 4. Hysteretic response of specimens

Hysteretic response

Figure 4-5 compares the hysteretic response of corroded and sound specimens. The maximum load capacity for the sound specimen in the north (negative direction) and south (positive direction) was 155 kN and 165 kN, respectively. Case 2 demonstrated 6% and 3.9% less maximum load capacity (MLC) in the positive and negative loading directions, respectively. However, Case 3 demonstrated remarkable improvements in MLC of 24% and 15.5% in the positive and negative loading directions, compared to the sound specimen. Compared to Case 2, the MLC increased by 32.3% and 20.1% in the positive and negative loading direction, respectively. It is noteworthy that the difference in MLC between the positive and negative directions was 12.7%, which can be attributed to cross-sectional non-uniform corrosion. Case 4 was subjected to 15% rebar corrosion, while the maximum load-carrying capacity was reduced by 9.2% and 6.5%, respectively, compared to the sound specimen in the positive and negative loading directions. However, Case 5 demonstrated 20% and 24% higher maximum load-carrying capacity in the positive and negative loading directions compared to the sound specimen.

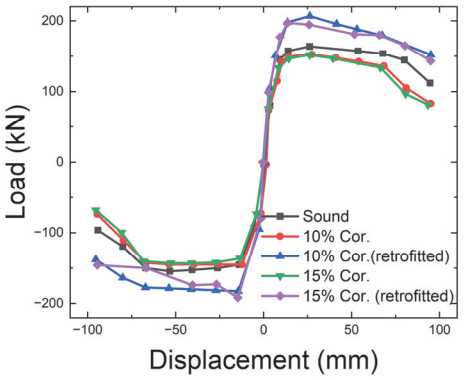

Figure 5. Backbone curve comparison of the sound, corroded, and strengthened specimens

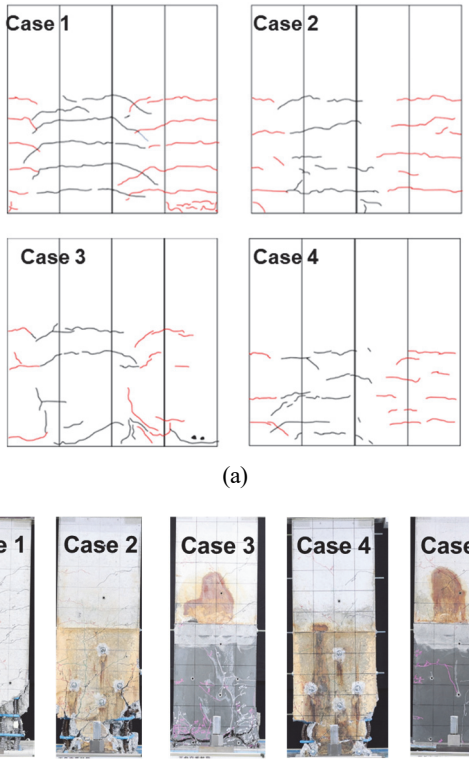

Figure 6. Comparison of crack pattern of the test specimens at (a) maximum lateral load and (b) final stage of loading

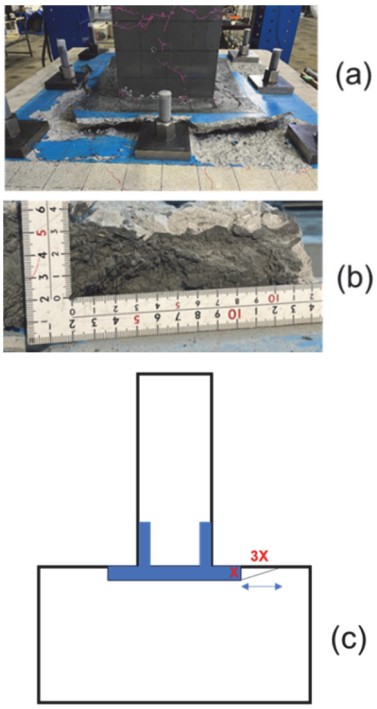

Figure 7. (a)　Photo of failed surface (b) UHPC layer thickness (c) Failure Analysis

Cracking patterns and failure modes

Crack propagation was recorded in every loading cycle. The cracking patterns of the test specimens at maximum lateral load and final stage are shown in Figure 6. As shown in Figure 6, the sound and corroded specimens demonstrate flexure dominant failure. The black and red lines represent cracks in the positive and negative loading cycles, respectively. In the sound specimen, the first flexural crack appears at the bottom at the lateral displacement of 3.5 mm. In the final stage of loading, the flexural cracks are distributed up to 900 mm from the bottom. These flexural cracks are distributed with an approximate spacing of 150 mm. The corroded specimens showed fewer cracks. The reason for this behaviour is the deterioration of the bond between the steel bar and the surrounding concrete. The increased lateral displacement results in significant spalling of the concrete cover. This behaviour can be attributed to the buckling of the longitudinal rebar and corrosion-induced cracking. Horizontal cracks resulted in flexure dominant failure in the sound and corroded specimens. The corroded specimens reinforced with the UHPC layers demonstrated greater control of crack propagation. Crack widths were notably smaller than with the sound and corroded specimen. Steel fibers in the UHPC matrix resulted in significant crack resistance due to bridge effects. In addition, the UHPC layers provided good confinement and resulted in less rebar buckling and spalling of the concrete cover. This behaviour helps achieve significant lateral resistance in UHPC-strengthened specimens.

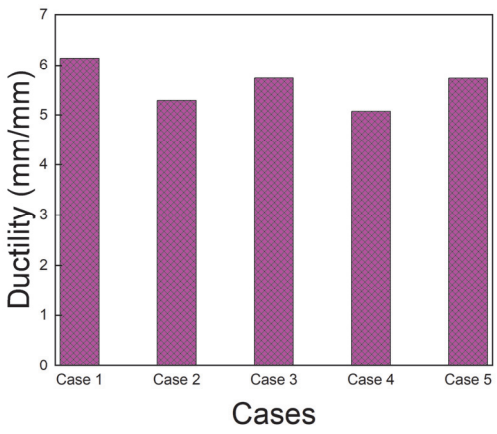

Figure 8. Comparison of ductility

Case 5 failed due to insufficient layer thickness, as shown in Figure 7. The desired layer thickness in this study was more than 60 mm. However, in Case 5, the average layer thickness was less than 50 mm. This result indicates that the UFC layers pushed against the surrounding concrete during reversed cyclic loading, resulting in tension and failure in the surrounding concrete. The results suggest that the length along which the tensile force is applied is about three times the thickness of the UFC layer. Based on these observations and depending on UFC layer thickness, the lateral load-resisting capacity of Case 5 can be calculated from the following equation, where X is the thickness of the UFC layer and $3X$ is the influence length. TSC is the tensile strength of concrete and LCL is the length of the UFC layer.

$$\text{Lateral load resisting capacity} = TSC \times LCL \times \sqrt{X^2 + (3X)^2} \quad (2)$$

Ductility

Rebar corrosion causes bond loss between rebar and concrete, reduces rebar cross sections, and generates spalling of the cover concrete. These factors reduce ductility. In this study, Case 2 and Case 4 demonstrated significantly less ductility than the sound specimen (see Figure 8). Ductility was reduced by 14% and 17% when Case 2 and Case 4 were subjected to 10% and 15% rebar corrosion, respectively. Interestingly, ductility was reduced by only about 7% in corroded specimens retrofitted with UHPC layers. This performance can be attributed to the steel fibers present in the UHPC and its superior material properties. Here, ductility is defined as the ratio between ultimate and yield displacement. Yield displacement is

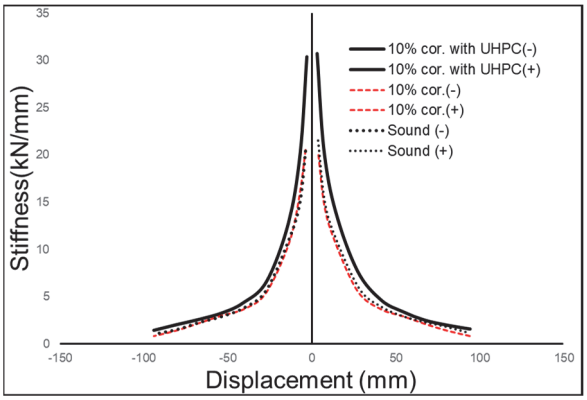

Figure 9. Stiffness degradation of sound and corroded specimens

determined by visual inspection (considering the change in stiffness); ultimate displacement corresponded to ultimate load (85% of MLC).

Stiffness degradation

A major goal of strengthening corroded RC bridge piers with UHPC layers is to improve stiffness. We evaluated the effects of UHPC layers on the stiffness of the corrosion-damaged bridge piers. Figure 9 shows the reduction in stiffness of the sound and corroded RC bridge piers during reversed cyclic loading. Here, stiffness is defined as K = load/deflection. The stiffness (K) of each cycle is determined by calculating the slope of the lines connecting the highest points of the loading. The figure shows the average of both the positive and negative loading cycles. As Figure 9 shows, the magnitude of the stiffness declines with greater deflection. Note that the corroded specimens strengthened with UHPC layers demonstrate significantly higher stiffness than the sound and corroded specimens. For example, at a deflection of 3.5 mm, Case 3 and Case 5 demonstrated about 33% and 31% higher stiffness than Case 2 and Case 4, respectively.

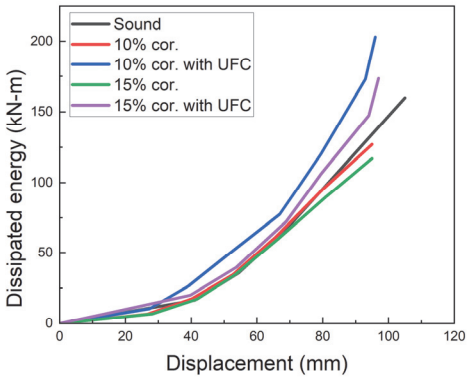

Figure 10.　Comparison of dissipated energy

Energy dissipation

We calculated the area in the hysteresis curve in a single loading cycle to determine the energy dissipation for sound, corroded, and retrofitted RC bridge piers. The energy dissipation capacity increases with the size of the enclosed area. Figure 10 illustrates the cumulative energy dissipation of the sound, corroded, and retrofitted specimens. As shown in Figure 10, hysteretic energy dissipation increases with greater deflection of the test specimen. Corrosion-damaged specimens retrofitted with UHPC layers demonstrate significantly higher energy dissipation than sound and corroded specimens. For example, Case 5 demonstrates approximately 100% higher cumulative energy dissipation capacity than Case 4, when displacement reaches 20 mm. Overall, Case 5 demonstrated 33% higher cumulative energy dissipation than Case 4. On the other hand, Case 3 displayed 59% higher cumulative energy dissipation capacity than Case 2.

CONCLUSIONS

This study proposes a flexural strengthening method for corrosion-damaged RC bridge piers using UHPC layers. In our study, Case 1 was a sound specimen; Cases 2 and 3 were subjected to 10% rebar corrosion; Cases 4 and 5 were subjected to 15% rebar corrosion. Cases 3 and 5 were retrofitted with UHPC layers measuring 50 mm in thickness. The following conclusions can be drawn from our study:

1. Strengthening corrosion-damaged RC bridge piers with UHPC layers is an effective repair option. Strengthened specimens demonstrate significantly higher cracking loads, yielding loads, and MLC. The strengthened specimens restored structural performance without affecting original geometry. In Case 3, MLC increased by 24% over the sound specimen.
2. RC bridge piers retrofitted with UHPC layers demonstrated significant crack control and increased durability.
3. RC bridge piers strengthened with UHPC layers demonstrated significantly higher initial stiffness than sound and corroded specimens. In the first loading cycle, Case 3 and Case 5 demonstrated about 33% and 31% higher stiffness than Case 2 and Case 4, respectively.
4. UHPC jacketing improves the displacement capacity or ductility of corroded specimens. Case 3 displayed 7.3% higher ductility than Case 2.

5. Energy dissipation capacity increased significantly when corroded specimens were strengthened with a UHPC jacket. Case 3 displayed 59% higher cumulative energy dissipation capacity than Case 2.

【References】

1) Biswas RK, Saito T, Misawa T, Iwanami M. Structural behavior of severely corroded RC beams retrofitted with UHPC layer: an experimental study. Innov Infrastruct Solut 2023;8:322.
2) Yuan W, Wang X, Guo A, Li C, Dong Z, Wu X. Cyclic performance of RC bridge piers retrofitted with UHPC jackets: Experimental investigation. Engineering Structures
3) Ali Dadvar S, Mostofinejad D, Bahmani H. Strengthening of RC columns by ultra-high performance fiber reinforced concrete (UHPFRC) jacketing. Construction and Building Materials 2020;235:117485.
4) JSCE, 2007. Standard Specifications for Concrete Structures